

# *Temperature thresholds of ecosystem respiration at a global scale.*

Article

Accepted Version

Johnston, A. S. A. ORCID: <https://orcid.org/0000-0001-8781-4039>, Meade, A., Ardö, J. ORCID: <https://orcid.org/0000-0002-9318-0973>, Arriga, N. ORCID: <https://orcid.org/0000-0001-5321-3497>, Black, A., Blanken, P. D. ORCID: <https://orcid.org/0000-0002-7405-2220>, Bonal, D. ORCID: <https://orcid.org/0000-0001-9602-8603>, Brümmer, C. ORCID: <https://orcid.org/0000-0001-6621-5010>, Cescatti, A., Dušek, J. ORCID: <https://orcid.org/0000-0001-6119-0838>, Graf, A. ORCID: <https://orcid.org/0000-0003-4870-7622>, Gioli, B. ORCID: <https://orcid.org/0000-0001-7631-2623>, Goded, I. ORCID: <https://orcid.org/0000-0002-1912-325X>, Gough, C. M. ORCID: <https://orcid.org/0000-0002-1227-7731>, Ikawa, H., Jassal, R. ORCID: <https://orcid.org/0000-0002-6727-5215>, Kobayashi, H. ORCID: <https://orcid.org/0000-0001-9319-0621>, Magliulo, V. ORCID: <https://orcid.org/0000-0001-5505-6552>, Manca, G. ORCID: <https://orcid.org/0000-0002-9376-0310>, Montagnani, L. ORCID: <https://orcid.org/0000-0003-2957-9071>, Moyano, F. E. ORCID: <https://orcid.org/0000-0002-4090-5838>, Olesen, J. E. ORCID: <https://orcid.org/0000-0002-6639-1273>, Sachs, T. ORCID: <https://orcid.org/0000-0002-9959-4771>, Shao, C., Tagesson, T. ORCID: <https://orcid.org/0000-0003-3011-1775>, Wohlfahrt, G. ORCID: <https://orcid.org/0000-0003-3080-6702>, Wolf, S. ORCID: <https://orcid.org/0000-0001-7717-6993>, Woodgate, W., Varlagin, A. ORCID:

<https://orcid.org/0000-0002-2549-5236> and Venditti, C.  
ORCID: <https://orcid.org/0000-0002-6776-2355> (2021)  
Temperature thresholds of ecosystem respiration at a global  
scale. *Nature Ecology & Evolution*, 5. pp. 487-494. ISSN 2397-  
334X doi: <https://doi.org/10.1038/s41559-021-01398-z>  
Available at <https://centaur.reading.ac.uk/96746/>

It is advisable to refer to the publisher's version if you intend to cite from the work. See [Guidance on citing](#).

To link to this article DOI: <http://dx.doi.org/10.1038/s41559-021-01398-z>

Publisher: Nature

All outputs in CentAUR are protected by Intellectual Property Rights law, including copyright law. Copyright and IPR is retained by the creators or other copyright holders. Terms and conditions for use of this material are defined in the [End User Agreement](#).

[www.reading.ac.uk/centaur](http://www.reading.ac.uk/centaur)

## **CentAUR**

Central Archive at the University of Reading

Reading's research outputs online

# 1 **Temperature thresholds of ecosystem respiration at a global scale**

2 Alice S.A. Johnston<sup>1,2\*</sup>, Andrew Meade<sup>2</sup>, Jonas Ardö<sup>3</sup>, Nicola Arriga<sup>4</sup>, Andy Black<sup>5</sup>, Peter D.  
3 Blanken<sup>6</sup>, Damien Bonal<sup>7</sup>, Christian Brümmer<sup>8</sup>, Alessandro Cescatti<sup>4</sup>, Jiří Dušek<sup>9</sup>, Alexander  
4 Graf<sup>10</sup>, Beniamino Gioli<sup>11</sup>, Ignacio Goded<sup>4</sup>, Christopher M. Gough<sup>12</sup>, Hiroki Ikawa<sup>13</sup>, Rachhpal  
5 Jassal<sup>5</sup>, Hideki Kobayashi<sup>14</sup>, Vincenzo Magliulo<sup>15</sup>, Giovanni Manca<sup>4</sup>, Leonardo  
6 Montagnani<sup>16,17</sup>, Fernando E. Moyano<sup>18</sup>, Jørgen E. Olesen<sup>19</sup>, Torsten Sachs<sup>20</sup>, Changliang  
7 Shao<sup>21</sup>, Torbern Tagesson<sup>22</sup>, Georg Wohlfahrt<sup>23</sup>, Sebastian Wolf<sup>24</sup>, William Woodgate<sup>25,26</sup>,  
8 Andrej Varlagin<sup>27</sup>, Chris Venditti<sup>2</sup>

9 <sup>1</sup> School of Water, Energy and Environment, Cranfield University, Bedfordshire, MK43 0AL, UK.

10 <sup>2</sup> School of Biological Sciences, University of Reading, Reading, RG6 6BX, UK.

11 <sup>3</sup> Physical Geography and Ecosystem Science, Lund University Sölvegatan 12, Sweden.

12 <sup>4</sup> European Commission, Joint Research Centre (JRC), Ispra, Italy.

13 <sup>5</sup> Faculty of Land and Food Systems; University of British Columbia; Vancouver, BC V6T 1Z4, Canada.

14 <sup>6</sup> Department of Geography, University of Colorado, Boulder CO, USA 80309-0260.

15 <sup>7</sup> Université de Lorraine, AgroParisTech, INRAE, UMR Silva, 54000 Nancy, France.

16 <sup>8</sup> Thünen Institute of Climate-Smart Agriculture, Bundesallee 65, 38116 Braunschweig, Germany.

17 <sup>9</sup> Global Change Research Institute of the Czech Academy of Sciences, CZ-60300 Brno, Czech Republic.

18 <sup>10</sup> Forschungszentrum Jülich, Institute for Bio- and Geosciences 3: Agrosphere, 52080 Jülich, Germany.

19 <sup>11</sup> CNR, Institute of Bioeconomy, 50145 Firenze, Italy.

20 <sup>12</sup> Virginia Commonwealth University, Department of Biology, Richmond, VA 23234, USA

21 <sup>13</sup> Institute for Agro-Environmental Sciences, National Agriculture and Food Research Organization, Tsukuba,  
22 305-8604, Japan

23 <sup>14</sup> Research Institute for Global Change, Institute of Arctic Climate and Environment Research, Japan Agency for  
24 Marine-Earth Science and Technology, Japan.

25 <sup>15</sup> CNR, Institute for Mediterranean Agriculture and Forest Systems, 85 80040 Ercolano, Italy.

26 <sup>16</sup> Autonomous Province of Bolzano, Forest Services, Bolzano 39100, Italy.

27 <sup>17</sup> Faculty of Science and Technology, Free University of Bolzano, Bolzano 39100, Italy

28 <sup>18</sup> University of Goettingen, Bioclimatology, Büsgenweg 2, 37077 Göttingen, Germany

29 <sup>19</sup> Aarhus University, Department of Agroecology, Blichers Allé 20, 8830 Tjele, Denmark

30 <sup>20</sup> GFZ German Research Centre for Geoscience, Telegrafenberg, Potsdam, Germany

31 <sup>21</sup> Institute of Agricultural Resources and Regional Planning, Chinese Academy of Agricultural Sciences, Beijing  
32 100081, China.

33 <sup>22</sup> Department of Geosciences and Natural Resources, University of Copenhagen, Øster Voldgade 10,  
34 Copenhagen, Denmark.

35 <sup>23</sup> Department of Ecology, University of Innsbruck, 6020 Innsbruck, Austria.

36 <sup>24</sup> Department of Environmental Systems Science, ETH Zurich, 8092 Zurich, Switzerland.

37 <sup>25</sup> Land & Water, Commonwealth Scientific and Industrial Research Organisation, 2601, Canberra, Australia

38 <sup>26</sup> School of Earth and Environmental Sciences, The University of Queensland, 4067, Queensland, Australia.

39 <sup>27</sup> A.N. Severtsov Institute of Ecology and Evolution, Russian Academy of Sciences, 119071, Leninsky pr.33,  
40 Moscow, Russia

41 \*Correspondence: [a.s.johnston@cranfield.ac.uk](mailto:a.s.johnston@cranfield.ac.uk)

## 42 **Abstract**

43 Ecosystem respiration is a major component of the global terrestrial carbon cycle and is  
44 strongly influenced by temperature. The global extent of the temperature-ecosystem  
45 respiration relationship, however, has not been fully explored. Here, we test linear and  
46 threshold models of ecosystem respiration across 210 globally distributed eddy covariance  
47 sites covering the most extensive temperature range ever studied. We find thresholds to the  
48 global temperature-ecosystem respiration relationship at high and low air temperatures and  
49 mid soil temperatures, which represent transitions in the temperature dependence and  
50 sensitivity of ecosystem respiration. Annual ecosystem respiration rates show a markedly  
51 reduced temperature dependence and sensitivity compared to half-hourly rates, and a single  
52 mid-temperature threshold for both air and soil temperature. Our study indicates a distinction  
53 in the influence of environmental factors, including temperature, on ecosystem respiration  
54 between latitudinal and climate gradients at short (half-hourly) and long (annual) timescales.  
55 Such climatological differences in the temperature sensitivity of ecosystem respiration have  
56 important consequences for the terrestrial net carbon sink under ongoing climate change.

## 57 **Main**

58 Carbon losses from terrestrial ecosystems determine the direction and magnitude of carbon-  
59 climate feedbacks<sup>1,2</sup>. The trajectory of future climate change therefore depends on the  
60 biological processes that underpin ecosystem fluxes. Ecosystem respiration ( $R_e$ ), the  
61 cumulative respiration of autotrophs (plants) and heterotrophs (bacteria, fungi and animals),  
62 represents a major component of the global carbon cycle<sup>3</sup>. Temperature strongly influences  
63  $R_e$  through the laws of thermodynamics<sup>4-6</sup>, but the global extent of the temperature- $R_e$   
64 relationship has not been fully explored<sup>7,8</sup>.

65 Temperature-mediated variations in  $R_e$  are typically described as an exponential function in  
66 Earth system models (ESMs)<sup>2</sup>. That is, globally static  $Q_{10}$  values of around 2 represent a  
67 doubling of ecosystem  $CO_2$  fluxes with an increase in temperature of 10 °C, when all other  
68 terms are equal<sup>9</sup>. Empirical and theoretical studies, however, have documented conflicting  
69 temperature- $R_e$  relationships. Latitudinal shifts in the temperature sensitivity of  $R_e$  have been  
70 observed in empirical studies, with ecosystems experiencing greater increases in  $R_e$  with  
71 temperature at high, compared to mid and low, latitudes<sup>8,10,11</sup>. At the same time, global  
72 syntheses have proposed convergent temperature sensitivities of  $R_e$  across different  
73 climates and ecosystem types<sup>4,12,13</sup>.

74 The influence of temperature on ecosystem respiration is mediated by the temperature  
75 sensitivity of individual physiology, community composition and biotic interactions of all the  
76 organisms inhabiting an ecosystem<sup>13,14</sup>. At the individual-level, metabolic rates scale with

77 body mass and increase exponentially with temperature according to the Boltzmann factor,  
78  $e^{-E/kT}$ , where  $E$  is the activation energy (eV),  $k$  is the Boltzmann's constant ( $8.62 \times 10^{-5}$  eV  
79  $K^{-1}$ ), and  $T$  is temperature (in Kelvin)<sup>6</sup>. Widescale application of the Boltzmann factor to  
80 individual metabolic rates has revealed a common value of  $E$  between 0.6 and 0.7 eV<sup>5,6,15</sup>. At  
81 the ecosystem-level, models based on metabolic theory indicate exponential temperature- $R_e$   
82 relationships across diverse ecosystems with a value of  $E$  surprisingly similar to individual  
83 metabolic rates (0.65 eV;  $Q_{10} \sim 2.50^{4,13}$ ). Yet, models of the temperature- $R_e$  relationship have  
84 focused on a limited temperature range between 0 and 30 °C, even though terrestrial  
85 ecosystems experience temperatures between -60 and 50 °C<sup>16</sup>.

86 In this study we test the generality of the temperature- $R_e$  relationship, described by a general  
87 ecosystem model, across the most extensive temperature range yet investigated. The  
88 model, founded in metabolic theory, gives the linear expression:

$$89 \quad \ln(R_e) = \frac{-E}{1,000k} \left( \frac{1,000}{T} \right) + \ln[(b_0)(C)] \quad (1)$$

90 where  $\ln(R_e)$  is the natural logarithm of ecosystem respiration, in  $W \text{ ha}^{-1}$ ;  $(1,000/T)$  is the  
91 reciprocal of absolute temperature;  $b_0$  is the intensity of cellular metabolism; and  $C$  is the  
92 size distribution of organisms (assumed to be independent of  $R_e$  according to the energy  
93 equivalence rule)<sup>4</sup>. The model predicts a general linear relationship between  $(1,000/T)$  and  
94  $\ln(R_e)$ , with an expected slope ( $\bar{E}$  from hereon in) across diverse ecosystems equal to -7.50  
95 K (0.65 eV, with a plausible range between -2 and -11 K, or 0.2 and 1.2 eV)<sup>10</sup>. However, we  
96 would expect climatological differences in resource supply<sup>17,18</sup> and community  
97 composition<sup>14,19</sup> to alter  $\bar{E}$  across the global temperature range. We would also expect  
98 divergent relationships between metabolism and resource supply with temperature to modify  
99 the temperature- $R_e$  relationship over time<sup>13,20</sup>.

## 100 **Results**

101 We test the global extent of the linear temperature- $R_e$  relationship predicted by metabolic  
102 theory, by applying the model presented in Eq. 1 to measurements across 210 globally  
103 distributed FLUXNET sites<sup>21</sup> (Figure 1 and Supplementary Data 1). Both short-term (half-  
104 hourly) and long-term (annual) measurements were tested for air and soil temperature. The  
105 half-hourly FLUXNET dataset is presented with more conventional temperature and  $R_e$  units  
106 in Extended Data 1. The linear model (Eq. 1) was compared to a threshold model, which  
107 accounts for variations in the activation energy ( $\bar{E}$ ) in Eq. 1 above and below specified  
108 temperature breakpoints (see Methods). That is, the threshold model accounts for shifts in  
109 the temperature sensitivity of  $R_e$  across the global temperature range, and explains  
110 latitudinal shifts in the temperature- $R_e$  relationship observed in empirical studies<sup>8,10,11</sup>. All

111 models were linear mixed effects models and goodness of fit comparisons used Akaike  
112 Information Criterion (AIC) measurements.

### 113 **Figure 1**

114 The threshold model, which integrated two temperature breakpoints of  $-24.8 \pm 0.15$  and  $15.1$   
115  $\pm 0.22$  °C, better explained  $R_e$  rates over the global extent of air temperatures in the  
116 FLUXNET dataset than the linear model ( $\Delta AIC = 3,839,265$ , Figure 2). Similar to previous  
117 findings<sup>4,13</sup>, the threshold model indicates a temperature sensitivity of  $R_e$  indistinguishable  
118 from that of  $-7.50$  K ( $0.65$  eV, dashed line in Figs. 2a & b) predicted by metabolic theory  
119 (likelihood ratio test:  $\chi^2 = 0$ ,  $p = 1$ ) between temperature breakpoints ( $\bar{E} = -7.42$  K,  $0.64$  eV,  
120  $Q_{10} \sim 2.45$  between  $15.1$  and  $-24.8$  °C, solid line in Fig. 2b). Evaluation of the linear model,  
121 on the other hand, gives an activation energy for global  $R_e$  rates of  $-7.30$  K ( $0.63$  eV, solid  
122 lines in Fig. 2a), significantly different from that predicted by metabolic theory (likelihood ratio  
123 test:  $\chi^2 = 20009$ ,  $p < 0.0001$ ). Importantly, the threshold model indicates a lower temperature  
124 sensitivity of  $R_e$  at higher temperatures ( $\bar{E} = -2.84$  K,  $0.25$  eV,  $Q_{10} \sim 1.41$  above  $15.1$  °C) and  
125 extreme temperature sensitivity of  $R_e$  at very low temperatures ( $\bar{E} = -30.53$  K,  $2.64$  eV,  $Q_{10} \sim$   
126  $40.79$  below  $-24.8$  °C). The threshold model therefore primarily improves predictions,  
127 compared to the linear model, of the temperature- $R_e$  relationship at low and high latitude  
128 sites (Figs. 2f & g). High measured variability in  $R_e$  across the global temperature range,  
129 however, likely reflects the interactive effects of disturbance events, plant phenology and soil  
130 water and nutrient limitation on ecosystem metabolism.

### 131 **Figure 2**

132 Given the importance of belowground communities in  $R_e$ <sup>14,19</sup>, linear and threshold models  
133 were tested for the global relationship between soil temperature and ecosystem respiration  
134 (Figure 2 and Supplementary Table 2). A single temperature threshold of  $11.4 \pm 0.29$  °C  
135 emerged for soil temperature, with little evidence for a lower temperature breakpoint  
136 (likelihood ratio test:  $\chi^2 = 0$ ,  $p = 1$ ). Above the temperature threshold, the activation energy of  
137  $R_e$  was lower than that observed for air temperature ( $\bar{E} = -2.18$  K,  $0.19$  eV,  $Q_{10} \sim 1.30$ ), while  
138 below the temperature threshold the activation energy was steeper than that between air  
139 temperature thresholds ( $\bar{E} = -13.37$  K,  $1.16$  eV,  $Q_{10} \sim 5.05$ ). The absence of a lower  
140 threshold for  $R_e$  with soil temperature is likely explained by thermal insulation from snow  
141 cover at low temperatures<sup>22</sup> resulting in much fewer observations, compared to air  
142 temperature, of the soil temperature- $R_e$  relationship below  $0$  °C.

143 To account for the relative uncertainties of eddy covariance measurements below  $-20$  °C<sup>23</sup>,  
144 alongside the emergence of a single temperature breakpoint for soil temperature, we tested  
145 the sensitivity of the air temperature threshold model to temperature ranges with few

146 available measurements (Extended Data 2). Ecosystem respiration data were classified in 5  
147 °C temperature intervals and intervals containing < 1% of all measurements (n < 235,521)  
148 were defined as low frequency intervals. Such intervals were present at both high (> 36 °C)  
149 and low (< -19 °C) temperatures. Each low frequency temperature interval was removed one  
150 by one, as well as all together (~ 1.8 % of the dataset), to investigate the sensitivity of the  
151 threshold model. The test provides supporting evidence of the robustness of temperature  
152 breakpoints to the removal of each temperature interval one by one. However, there was no  
153 support for a lower temperature breakpoint (-24.8 °C in Fig. 2b & c) when all low frequency  
154 intervals or all those < -19 °C were removed. Instead, a single temperature breakpoint of  
155 14.6 °C emerged (Extended Data 3 and Supplementary Table 3). The lower air temperature  
156 breakpoint should therefore be considered with caution until more accurate  $R_e$   
157 measurements at low temperatures can be made.  $R_e$  rates nevertheless display a sharp  
158 decline at lower temperatures for both air (Fig. 2b) and soil (Fig. 3b) temperatures.

### 159 **Figure 3**

160 Sharp declines in  $R_e$  at low soil and air temperatures likely indicate pulse responses of soil  
161 respiration to rewetting and thawing events<sup>24</sup>, attributed to the suppression of microbial  
162 activity under water limitation in freezing conditions<sup>25</sup> and an uncoupling of the temperature  
163 dependence of microbial respiration from thermodynamic laws<sup>26</sup>. Differences between global  
164 temperature- $R_e$  relationships for air and soil temperature at short timescales also suggest  
165 shifts in the contribution of aboveground and belowground communities to  $R_e$  across the  
166 global extent of temperatures. For instance, a lower activation energy for the temperature- $R_e$   
167 relationship at higher soil temperatures ( $\bar{E} = -2.18 \text{ K} > 11.4 \pm 0.29 \text{ °C}$ , Fig. 3), compared to air  
168 temperatures ( $\bar{E} = -2.84 \text{ K} > 15.1 \text{ °C}$ , Fig. 2), could indicate a relative reduction in the  
169 contribution of belowground autotrophs and heterotrophs to  $R_e$  in warmer climates. On the  
170 other hand, the lower threshold for the temperature- $R_e$  relationship at low air temperatures  
171 could reflect a temperature limit for the metabolism of aboveground communities, whereas  
172 the absence of a lower temperature threshold for soil temperature suggests the importance  
173 of belowground communities as components of  $R_e$  in mild to cold climates.

174 Global air temperature thresholds were consistent across climates, but the goodness of fit of  
175 the threshold model (pseudo  $r^2$  and  $\Delta\text{AICs}$  compared to the linear model, Fig. 4) declined  
176 with a decrease in overall temperature range at lower latitudes. For instance, the  
177 temperature dependence of  $R_e$  (variation in  $R_e$  rates explained by temperature) was greater  
178 in cold, higher latitude, climates (tundra and boreal,  $r_m^2 > 0.60$ ), compared to mild  
179 (temperate,  $r_m^2 = 0.48$ ) and warm, low latitude, climates (mediterranean and tropical,  $r_m^2 \leq$   
180 0.09). In warmer climates, random effects had a much greater influence on  $R_e$  than in mild or  
181 cold climates, with FLUXNET site and latitude explaining more variation in tropical and

182 mediterranean ecosystems (Supplementary Table 4). Across the 210 sites, the threshold  
183 model better predicted the temperature- $R_e$  relationship in the majority of cases ( $n = 197$ ,  
184 Supplementary Data 1), while temperature explained more of the variation in  $R_e$  rates at  
185 sites with greater temperature ranges and higher latitudes (and Extended Data 4).

186  $Q_{10}$  estimates from the threshold model reflect latitudinal shifts in the temperature sensitivity  
187 of ecosystem respiration, with tropical, mediterranean, temperate, boreal, and tundra  
188 climates yielding  $Q_{10}$  values of  $1.38 \pm 0.01$ ,  $1.82 \pm 0.43$ ,  $2.32 \pm 0.31$ ,  $2.67 \pm 0.10$ , and  $2.90$   
189  $\pm 0.12$  respectively, compared to a global  $Q_{10}$  of  $2.26 \pm 0.35$ , and higher  $Q_{10}$  estimates based  
190 on the soil temperature threshold model (Supplementary Table 5). Empirical observations of  
191  $R_e$ , soil respiration and carbon turnover rates are comparable with threshold model  
192 estimates of higher temperature sensitivities of  $R_e$  at high-latitudes and lower temperature  
193 sensitivities of  $R_e$  at low-latitudes<sup>10,27</sup>. Weaker temperature control in the linear model, similar  
194 to ESMs that implement static global  $Q_{10}$  values, cannot capture shifts in  $R_e$  temperature  
195 sensitivities across the global temperature range (Supplementary Table 5).

#### 196 **Figure 4**

197 Annual temperature- $R_e$  relationships were analysed across site years to investigate whether  
198 climatological differences in the temperature dependence and sensitivity of  $R_e$  emerge over  
199 longer timescales. The threshold model explained the temperature- $R_e$  relationship better  
200 than the linear model at longer timescales for both air and soil temperature (Fig. 5).  
201 Surprisingly, threshold models converged for air and soil temperature, with a single mid-  
202 temperature breakpoint of  $11.0 \pm 0.16$  °C (Figs 5b & d). Above the temperature threshold,  
203 annual  $R_e$  rates declined with increasing mean annual temperatures from mid to low  
204 latitudes, while the activation energy below the temperature threshold was markedly reduced  
205 (Figs 5a & c,  $\bar{E} \sim -4.90$  K, 0.42 eV) compared to short timescales. Weaker temperature  
206 relationships at longer timescales is reflected by global  $Q_{10}$  estimates of  $1.34 \pm 0.55$  and  $1.29$   
207  $\pm 0.58$  for air and soil temperature, respectively (Supplementary Table 6). An overall lack of  
208  $R_e$  variation explained by temperature ( $r^2_m < 0.14$ ) likely reflects the importance of  
209 confounding effects from soil water, nutrient limitation, and resource availability, alongside  
210 thermal acclimation, at longer timescales. The threshold model was further consistent for  
211 annual soil respiration and air temperature measurements from the Global Soil Respiration  
212 Database<sup>28</sup>, with a single temperature breakpoint of 5.5 °C (Extended Data 5 and  
213 Supplementary Table 6).

#### 214 **Figure 5**

215



## 216 Discussion

217 Our study shows how latitudinal shifts in  $R_e$  temperature sensitivity at both short and long  
218 timescales correspond to transitions in the global temperature– $R_e$  relationship across  
219 temperature thresholds. Importantly, temperature thresholds also indicate differences in the  
220 temperature dependence of  $R_e$ , with more variation in  $R_e$  rates explained by temperature in  
221 cold compared to warm climates. In cold climates, temperature strongly influences metabolic  
222 activity of belowground microbial communities<sup>19,25,26</sup>. In warm climates, ecosystem  
223 metabolism is limited by water and nutrient availability, and resource availability to biological  
224 communities<sup>18,27,29–31</sup>.

225 Both the temperature sensitivity and dependence of annual  $R_e$  rates is markedly reduced  
226 compared to the short-term  $R_e$  temperature response, suggesting the dominance of resource  
227 effects on ecosystem metabolism at longer timescales<sup>13</sup>. For instance, primary production  
228 directs carbon availability for ecosystem metabolism and typically shows a weaker  
229 temperature dependence<sup>20,32</sup>. Nutrient availability further drives preferential allocation of  
230 photosynthate C above- or below-ground, with consequences for carbon availability and  
231 quality to different ecosystem components<sup>17</sup>.

232 Thresholds to the temperature– $R_e$  relationship shown here will undoubtedly result from  
233 temporally divergent sensitivities between ecosystem components (e.g. below- and above-  
234 ground, heterotrophic and autotrophic) and several environmental controls over time.  
235 Variable acclimation of the different components of  $R_e$  to these environmental controls may  
236 further influence the temperature dependence and sensitivity of  $R_e$  by modifying the  
237 temperature response of catabolic and anabolic pathways<sup>33–35</sup>. Although we would expect  
238 such mechanisms to occur as gradual state changes rather than the sharp breakpoints  
239 described here, our study indicates consistent temperature thresholds at which ecosystem  
240 metabolism changes at a global scale. However, such results need to be validated for  
241 different ecosystem components as detailed measurements become available, and for  
242 decadal timescales over which the influence of anthropogenic factors can be detected.

243 Biosphere feedbacks with future climate changes will be strongly influenced by the  
244 temperature– $R_e$  relationship<sup>36,37</sup> and latitudinal shifts in  $R_e$  temperature sensitivity as  
245 identified here will have important consequences for the global net land carbon sink<sup>38</sup>. For  
246 instance, while huge stores of labile carbon in permafrost regions could be released if  
247 temperatures rise above lower thresholds for microbial decomposition<sup>26</sup>, CO<sub>2</sub> fertilisation in  
248 tropical and boreal regions could enhance carbon gains through primary production relative  
249 to losses through  $R_e$ <sup>30,39</sup>. Climate change forecasts by ESMs would thus be improved by  
250 accounting for temperature thresholds of  $R_e$  at a global scale. A higher resolution

251 understanding of  $R_e$ -climate feedbacks, however, requires strategic disentangling of the  
252 multiple environmental controls on the aboveground, belowground, heterotrophic, and  
253 autotrophic components of terrestrial ecosystem carbon fluxes.

## 254 **Methods**

### 255 **The FLUXNET dataset**

256 FLUXNET is a global network of micrometeorological sites providing eddy covariance CO<sub>2</sub>  
257 exchange observations between terrestrial ecosystems and the atmosphere<sup>21</sup>. The  
258 FLUXNET 2015 dataset used in this study provides half hourly temperature and night-time  
259  $R_e$  measurements over 1454 site years and a latitudinal range of 78.92 °N to 37.43 °S.  
260 Observations across the 210 sites, which range from arctic tundra to tropical rainforest  
261 ecosystems, provide an extensive temperature range of 89.7 °C, from -43.4 to 46.3 °C  
262 (Figure 1 and Supplementary Data 1).

263 The FLUXNET dataset is subject to a data processing pipeline which include data quality  
264 controls checks, filtering of low turbulence periods and partitioning of CO<sub>2</sub> fluxes into  
265 respiration and photosynthesis components using established methods<sup>21</sup>. Disentangling  
266 respiration and photosynthesis fluxes during the day is complex and the extraction of  $R_e$   
267 relies on modelling techniques with high uncertainty. Night-time CO<sub>2</sub> exchange  
268 measurements thus provide the best approximation of  $R_e$ , and uncertainty has been  
269 minimised for the FLUXNET dataset by employing quality control procedures<sup>21</sup>. Here, non-  
270 gap-filled half hourly ( $\mu\text{mol CO}_2 \text{ m}^{-2} \text{ s}^{-1}$ ) and annual ( $\text{g C m}^{-2}$ ) night-time  $R_e$   
271 (RECO\_NT\_VUT\_MEAN), air temperature (TA\_F) and soil temperature (TS\_F)  
272 measurements were compiled from the FLUXNET 2015 dataset  
273 (<https://fluxnet.fluxdata.org/data/fluxnet2015-dataset/>).  $R_e$  measurements were then  
274 converted to units of metabolic energy ( $\text{W ha}^{-1}$ )<sup>4</sup> by taking 0.272 J  $\mu\text{mol CO}_2$  and 10,000  $\text{m}^2$   
275  $\text{ha}^{-1}$ .

### 276 **Model analysis**

277 The linear model (1) for describing the temperature- $R_e$  relationship was fitted to the global  
278 FLUXNET dataset, for both air and soil temperature. To test for the presence of temperature  
279 thresholds to the linear temperature- $R_e$  model at a global scale, which explain shifts in  $R_e$   
280 temperature sensitivity across climates, we compare the linear model in Eq. 1 to a threshold  
281 (piecewise) model. The threshold model, with two temperature breakpoints, gives:

$$282 \quad \ln(R_e) = \bar{E}_1 f_1(1,000/T, k_1) + \bar{E}_2 f_2(1,000/T, k_1, k_2) k_2 + \bar{E}_3 f_3(1,000/T, k_2) + \ln[(b_0)(C)] \quad (2)$$

283 where  $\bar{E}_1$ ,  $\bar{E}_2$  and  $\bar{E}_3$  represent activation energies for different temperature ( $1,000/T$ ) ranges,  
284 determined by the two temperature breakpoints ( $k_1$  and  $k_2$ ) and  $f$  represents the functions:

285

286

$$f_1 = \begin{cases} 1,000/T, & 1,000/T \leq k_1 \\ k_1, & k_1 > 1,000/T \end{cases}$$

287

$$f_2 = \begin{cases} 0, & 1,000/T \leq k_1 \\ 1,000/T - k_1, & k_1 \leq 1,000/T \leq k_2 \\ k_2 - k_1, & 1,000/T > k_2 \end{cases}$$

288

$$f_3 = \begin{cases} 0, & 1,000/T \leq k_2 \\ 1,000/T, & 1,000/T > k_2 \end{cases}$$

289 The threshold model first introduced a single temperature breakpoint to the linear model, so  
290 that the activation energy ( $\bar{E}$ , with more negative values indicating higher temperature  
291 sensitivity) varies above and below a specified temperature. Temperature breakpoints were  
292 tested for the temperature ( $1,000/T$ ) range between 3.1 and 4.4, for every increment of 0.001  
293 ( $\sim 0.07$  °C). Differences in linear and threshold model AIC's were then compared for every  
294 temperature breakpoint. The highest  $\Delta$ AIC was taken as providing the most support for a  
295 temperature breakpoint, as long as  $\Delta$ AIC  $> 5$  for additional degrees of freedom and  $p < 0.05$   
296 in a likelihood ratio test. Then, the threshold model integrated an additional temperature  
297 breakpoint, taking the first temperature breakpoint with the greatest support as a fixed  
298 value. Model AIC's for each second temperature breakpoint were compared to the single  
299 threshold model and the second threshold was selected based on the highest  $\Delta$ AIC given  
300 the conditions outlined above. Temperature breakpoints were identified for short (half-hourly)  
301 and long (annual) temperature- $R_e$  relationships.

302 All models were linear mixed effects models, with FLUXNET site and latitude set as random  
303 effects. First, the models were tested for the global dataset and then for broadly classified  
304 climate zones (cold, mild, and warm) and climates (tundra, boreal, temperate,  
305 mediterranean, and tropical). Some generalisations were necessary during climate  
306 classification. For instance, alpine sites at mid-latitudes were classified as boreal climates  
307 (Supplementary Data 1). Linear and threshold models were further tested for each  
308 FLUXNET site. Finally, annual  $R_e$  rates were used to investigate changes in temperature  
309 breakpoints, and linear and threshold model performance, at long timescales for air and soil  
310 temperature. Long timescale models accounted for latitude and year as random effects.

## 311 **References**

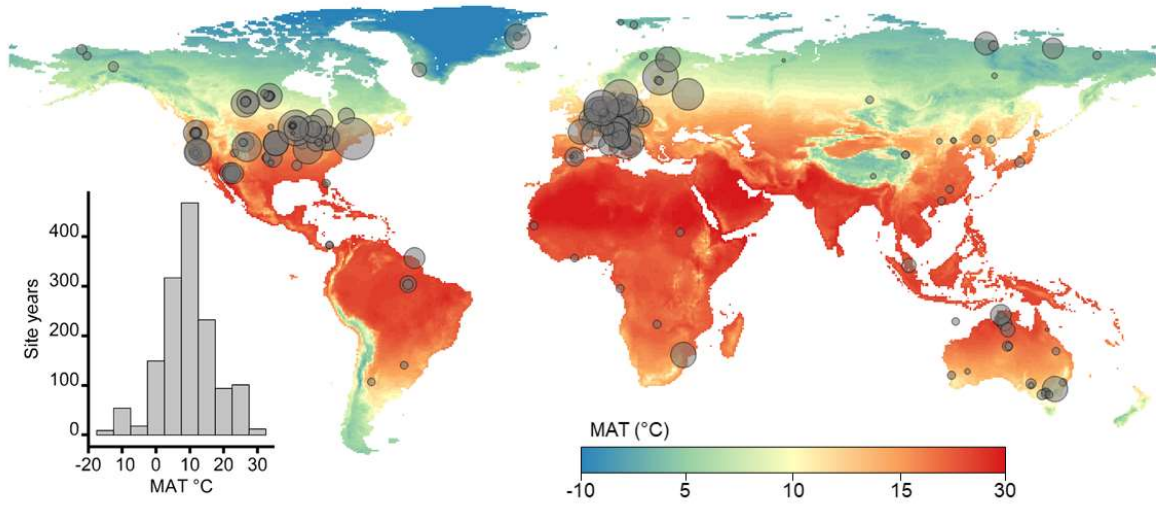
- 312 1. Cao, M. & Woodward, F. I. Dynamic responses of terrestrial ecosystem carbon cycling to  
313 global climate change. *Nature* **393**, 249–252 (1998).

- 314 2. Heimann, M. & Reichstein, M. Terrestrial ecosystem carbon dynamics and climate  
315 feedbacks. *Nature* **451**, 289–292 (2008).
- 316 3. Allen, A. P., Gillooly, J. F. & Brown, J. H. Linking the global carbon cycle to individual  
317 metabolism. *Funct. Ecol.* **19**, 202–213 (2005).
- 318 4. Enquist, B. J. *et al.* Scaling metabolism from organisms to ecosystems. *Nature* **423**,  
319 639–642 (2003).
- 320 5. Gillooly, J. F., Brown, J. H., West, G. B., Savage, V. M. & Charnov, E. L. Effects of size  
321 and temperature on metabolic rate. *Science* **293**, 2248–2251 (2001).
- 322 6. Brown, J. H., Gillooly, J. F., Allen, A. P., Savage, V. M. & West, G. B. Toward a  
323 metabolic theory of ecology. *Ecology* **85**, 1771–1789 (2004).
- 324 7. Friedlingstein, P. *et al.* Uncertainties in CMIP5 climate projections due to carbon cycle  
325 feedbacks. *J. Clim.* **27**, 511–526 (2014).
- 326 8. Davidson, E. A. & Janssens, I. A. Temperature sensitivity of soil carbon decomposition  
327 and feedbacks to climate change. *Nature* **440**, 165–173 (2006).
- 328 9. Lenton, T., M. & Huntingford, C. Global terrestrial carbon storage and uncertainties in its  
329 temperature sensitivity examined with a simple model. *Glob. Change Biol.* **9**, 1333–1352  
330 (2003).
- 331 10. Song, B. *et al.* Divergent apparent temperature sensitivity of terrestrial ecosystem  
332 respiration. *J. Plant Ecol.* **7**, 419–428 (2014).
- 333 11. Lloyd, J. & Taylor, J. A. On the temperature dependence of soil respiration. *Funct. Ecol.*  
334 315–323 (1994).
- 335 12. Mahecha, M. D. *et al.* Global Convergence in the Temperature Sensitivity of Respiration  
336 at Ecosystem Level. *Science* **329**, 838–840 (2010).
- 337 13. Yvon-Durocher, G. *et al.* Reconciling the temperature dependence of respiration across  
338 timescales and ecosystem types. *Nature* **487**, 472–476 (2012).
- 339 14. Johnston, A. S. A. & Sibly, R. M. The influence of soil communities on the temperature  
340 sensitivity of soil respiration. *Nat. Ecol. Evol.* **2**, 1597–1602 (2018).

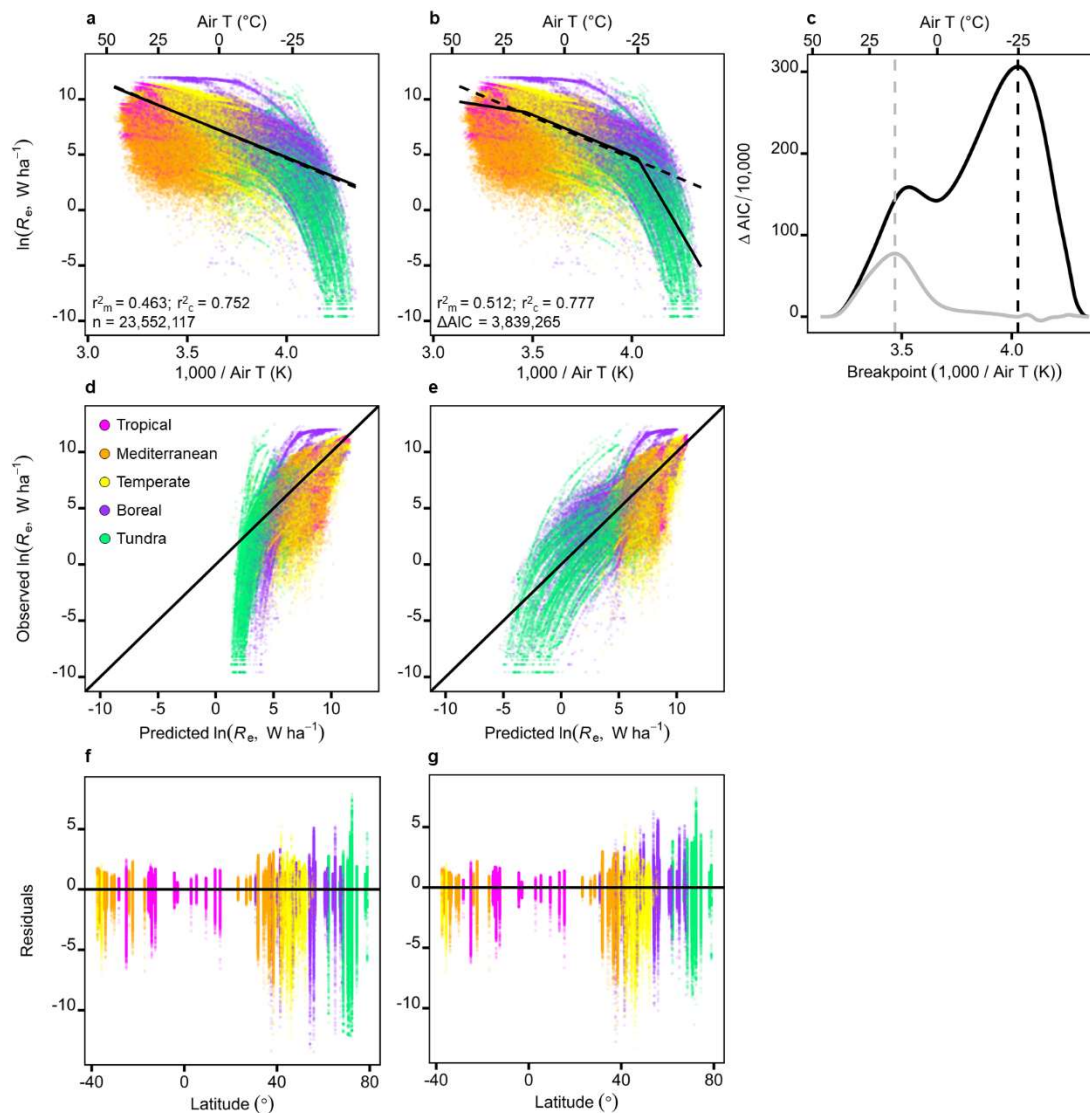
- 341 15. Dell, A. I., Pawar, S. & Savage, V. M. Systematic variation in the temperature  
342 dependence of physiological and ecological traits. *Proc. Natl. Acad. Sci.* **108**, 10591–  
343 10596 (2011).
- 344 16. Buckley, L. B. & Huey, R. B. Temperature extremes: geographic patterns, recent  
345 changes, and implications for organismal vulnerabilities. *Glob. Change Biol.* **22**, 3829–  
346 3842 (2016).
- 347 17. Gill, A. L. & Finzi, A. C. Belowground carbon flux links biogeochemical cycles and  
348 resource-use efficiency at the global scale. *Ecol. Lett.* **19**, 1419–1428 (2016).
- 349 18. Green, J. K. *et al.* Large influence of soil moisture on long-term terrestrial carbon uptake.  
350 *Nature* **565**, 476–479 (2019).
- 351 19. Allison, S. D., Wallenstein, M. D. & Bradford, M. A. Soil-carbon response to warming  
352 dependent on microbial physiology. *Nat. Geosci.* **3**, 336–340 (2010).
- 353 20. Michaletz, S. T., Cheng, D., Kerkhoff, A. J. & Enquist, B. J. Convergence of terrestrial  
354 plant production across global climate gradients. *Nature* **512**, 39–43 (2014).
- 355 21. Pastorello, G. *et al.* The FLUXNET2015 dataset and the ONEFlux processing pipeline  
356 for eddy covariance data. *Sci. Data* **7**, 225 (2020).
- 357 22. Monson, R. K. *et al.* Winter forest soil respiration controlled by climate and microbial  
358 community composition. *Nature* **439**, 711–714 (2006).
- 359 23. Mauder, M. *et al.* A strategy for quality and uncertainty assessment of long-term eddy-  
360 covariance measurements. *Agric. For. Meteorol.* **169**, 122–135 (2013).
- 361 24. Kim, D.-G., Vargas, R., Bond-Lamberty, B. & Turetsky, M. R. Effects of soil rewetting  
362 and thawing on soil gas fluxes: a review of current literature and suggestions for future  
363 research. *Biogeosciences* **9**, 2459–2483 (2012).
- 364 25. Du, E. *et al.* Winter soil respiration during soil-freezing process in a boreal forest in  
365 Northeast China. *J. Plant Ecol.* **6**, 349–357 (2013).
- 366 26. Schuur, E. A. *et al.* Climate change and the permafrost carbon feedback. *Nature* **520**,  
367 171–179 (2015).

- 368 27. Koven, C. D., Hugelius, G., Lawrence, D. M. & Wieder, W. R. Higher climatological  
369 temperature sensitivity of soil carbon in cold than warm climates. *Nat. Clim. Change* **7**,  
370 817–822 (2017).
- 371 28. Bond-Lamberty, B. P. & Thomson, A. M. A Global Database of Soil Respiration Data,  
372 Version 4.0. *ORNL DAAC* (2018) doi:<https://doi.org/10.3334/ORNLDAAAC/1578>.
- 373 29. Zhang, Z. *et al.* A temperature threshold to identify the driving climate forces of the  
374 respiratory process in terrestrial ecosystems. *Eur. J. Soil Biol.* **89**, 1–8 (2018).
- 375 30. Yang, Y., Donohue, R. J., McVicar, T. R., Roderick, M. L. & Beck, H. E. Long-term CO<sub>2</sub>  
376 fertilization increases vegetation productivity and has little effect on hydrological  
377 partitioning in tropical rainforests. *J. Geophys. Res. Biogeosciences* **121**, 2125–2140  
378 (2016).
- 379 31. Fleischer, K. *et al.* Amazon forest response to CO<sub>2</sub> fertilization dependent on plant  
380 phosphorus acquisition. *Nat. Geosci.* **12**, 736–741 (2019).
- 381 32. Padfield, D. *et al.* Metabolic compensation constrains the temperature dependence of  
382 gross primary production. *Ecol. Lett.* **20**, 1250–1260 (2017).
- 383 33. Atkin, O. K. & Tjoelker, M. G. Thermal acclimation and the dynamic response of plant  
384 respiration to temperature. *Trends Plant Sci.* **8**, 343–351 (2003).
- 385 34. Huntingford, C. *et al.* Implications of improved representations of plant respiration in a  
386 changing climate. *Nat. Commun.* **8**, 1602 (2017).
- 387 35. Niu, S. *et al.* Thermal optimality of net ecosystem exchange of carbon dioxide and  
388 underlying mechanisms. *New Phytol.* **194**, 775–783 (2012).
- 389 36. Rind, D. The Consequences of Not Knowing Low- and High-Latitude Climate Sensitivity.  
390 *Bull. Am. Meteorol. Soc.* **89**, 855–864 (2008).
- 391 37. Liu, Z. *et al.* Increased high-latitude photosynthetic carbon gain offset by respiration  
392 carbon loss during an anomalous warm winter to spring transition. *Glob. Change Biol.*  
393 **26**, 682–696 (2020).
- 394 38. Haverd, V. *et al.* Higher than expected CO<sub>2</sub> fertilization inferred from leaf to global  
395 observations. *Glob. Change Biol.* **26**, 2390–2402 (2020).

396 39. Tagesson, T. *et al.* Recent divergence in the contributions of tropical and boreal forests  
397 to the terrestrial carbon sink. *Nat. Ecol. Evol.* **4**, 202–209 (2020).  
398

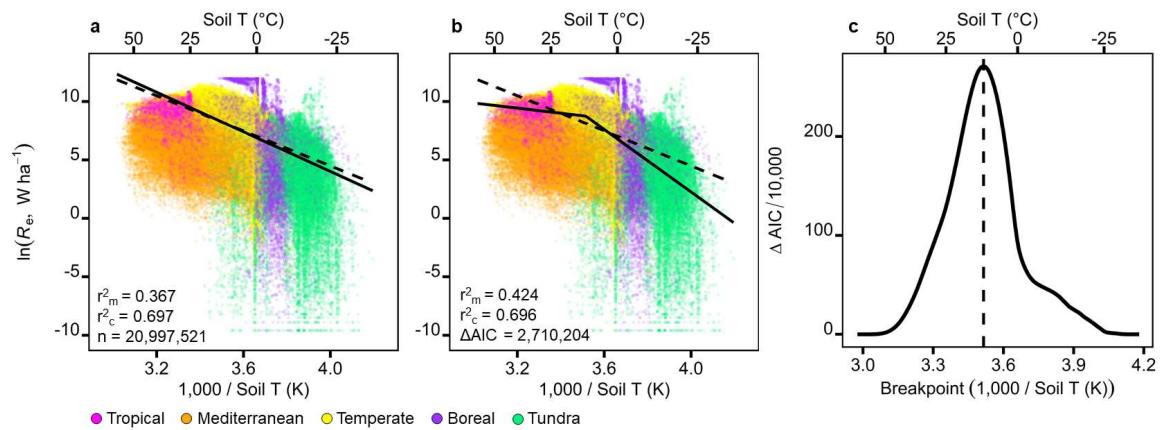


399 **Figure 1. Global distribution of the FLUXNET sites.** Site locations (n = 210) are displayed over a  
400 world mean annual temperature (MAT) map. Symbol diameter represents the number of site years  
401 (range: 1 to 22 years) and the inset left-hand figure shows the distribution of site years (n = 1454) by  
402 MAT.  
403



404  
 405 **Figure 2. Global extent of the temperature-ecosystem respiration ( $R_e$ ) relationship.** Night-time  
 406 half hourly ecosystem respiration measurements from the FLUXNET dataset (symbols), broadly  
 407 classified as tropical (magenta), mediterranean (orange), temperate (yellow), boreal (purple) or tundra  
 408 (green) climates. Left-hand plots (a, d & f) present predictions from the linear model (Eq. 1) and  
 409 middle plots (b,e & g) from a threshold model with two temperature breakpoints (Eq. 2), of the  
 410 temperature-ecosystem respiration relationship. The right-hand plot (c) shows the presence of two  
 411 temperature breakpoints (black line: air  $(1,000/T)= 4.027$ ,  $-24.8$  °C; grey line: air  $(1,000/T) = 3.469$ ,  
 412  $15.1$  °C), identified by the threshold models performance ( $\Delta AIC$ 's compared to the linear model where  
 413 higher values provide a better fit to the FLUXNET dataset). Goodness of fit measures indicate the  
 414 pseudo  $r^2$  for marginal (fixed) effects ( $r^2_m$ ) and conditional (fixed and random) effects ( $r^2_c$ ), with top  
 415 plots (a & b) showing predictions of the fixed effects only (temperature, solid lines) in each model  
 416 compared to the activation energy of  $-7.50$  K predicted by metabolic theory (dashed lines,  $r^2_m = 0.361$ ;  
 417  $r^2_c = 0.542$ ). Middle plots (d & e) present model predictions against observed FLUXNET  
 418 measurements (solid black 1:1 lines would demonstrate perfect prediction), and bottom plots (f & g)  
 419 show model residuals against latitude. Full details of the linear mixed effects models are presented in  
 420 Supplementary Table 1.





421

422

**Figure 3. The global soil temperature-ecosystem respiration relationship.** Night-time half hourly

423

ecosystem respiration measurements from the FLUXNET dataset (symbols), broadly classified by

424

climate with symbol colours as in Figure 2. Predictions of the temperature-ecosystem respiration

425

relationship are compared for a) the linear model and b) the threshold model, for the fixed effects of

426

temperature (solid lines). Both models are compared to the activation energy of -7.50 K predicted by

427

metabolic theory (dashed lines,  $r_m^2 = 0.173$ ,  $r_c^2 = 0.500$ ). The right-hand plot (c) shows the presence of

428

a single temperature breakpoints (black line: soil ( $1,000/T$ ) = 3.515, 11.4  $^\circ\text{C}$ ), identified by the

429

threshold models performance ( $\Delta\text{AIC}$ 's compared to the linear model where higher values provide a

430

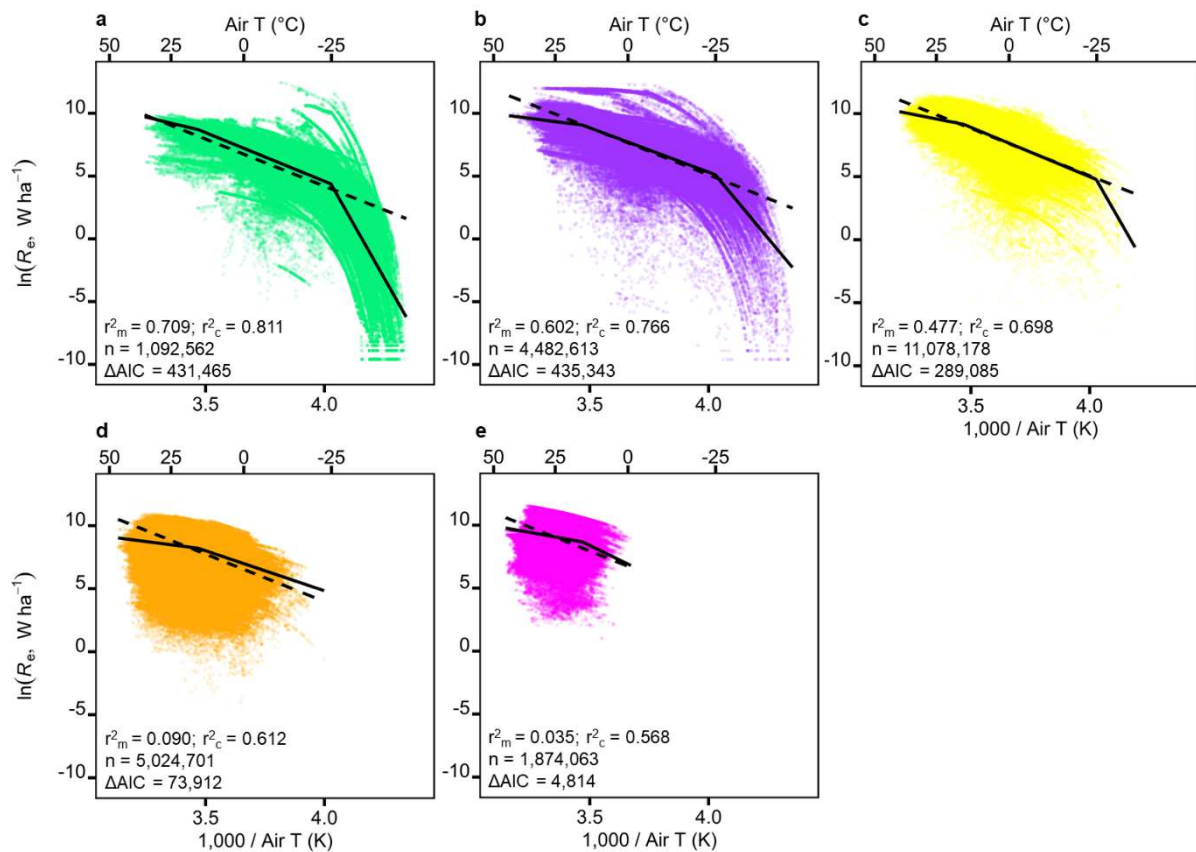
better fit to the FLUXNET dataset). Full details of the linear mixed effects models are presented in

431

Supplementary Table 2.

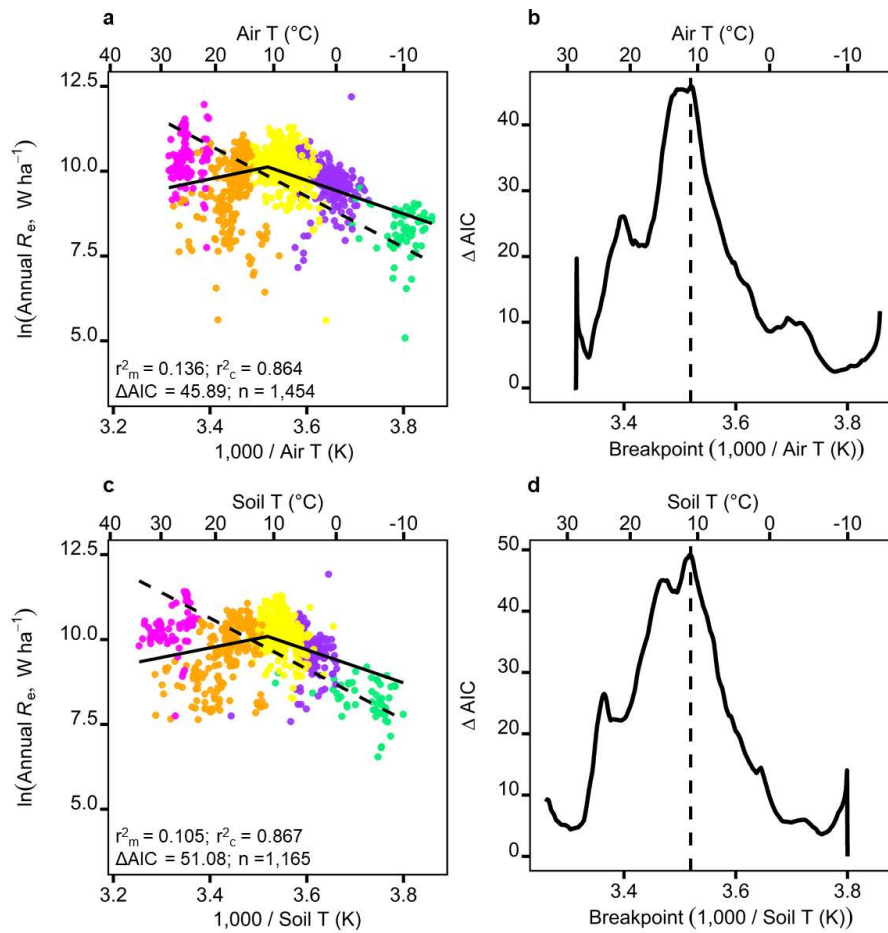
432

432



434

435 **Figure 4. Temperature thresholds of ecosystem respiration ( $R_e$ ) across five climates.** Night-time  
 436 half hourly ecosystem respiration measurements from the FLUXNET dataset (symbols), classified as  
 437 a) tundra, b) boreal), c) temperate, d) mediterranean, and e) tropical, with symbol colours as in Figure  
 438 2. Solid lines show threshold model predictions for the fixed effects of temperature, and dashed lines  
 439 show an activation energy of -7.5 K predicted by metabolic theory.  $\Delta AICs$  indicate a greater goodness  
 440 of fit of the threshold compared to linear model. Full details of the linear mixed effects models are  
 441 presented in Supplementary Table 4.



442

443 **Figure 5. Long-term temperature thresholds of ecosystem respiration ( $R_e$ ).** Mean annual  $R_e$  and  
 444 either a) air or c) soil temperature measurements (symbols), with symbol colours representing climate  
 445 as in Figure 2. Plots show predictions from the threshold model (solid lines, for the fixed effects of  
 446 temperature only). Both threshold models identified a single temperature breakpoint of 11.0 °C, with  
 447 little support for a second temperature breakpoint ( $\Delta AIC < 5$  and  $p > 0.05$ ). Dashed lines indicate an  
 448 activation energy of -7.50 K as predicted by metabolic theory and  $\Delta AICs$  are between the linear and  
 449 threshold models. Full details of the threshold mixed effects models are presented in Supplementary  
 450 Table 6.

#### 451 **Data availability**

452 The dataset analysed during the current study is available on Dryad  
 453 (<https://doi.org/10.5061/dryad.70rxwdbwk>).

#### 454 **Code availability**

455 The R code used for analysis during the current study is available on Dryad  
 456 (<https://doi.org/10.5061/dryad.70rxwdbwk>).

457

458 **Acknowledgements**

459 This work used eddy covariance data acquired and shared by the FLUXNET community and  
460 was supported by a Leverhulme Trust Research Project Grant (RPG-2017-071) and a  
461 Leverhulme Trust Research Leadership Award (RL-2019-012) to CV. AM was supported by  
462 BBSRC (BB/S019952/1) and the Leverhulme Trust (RPG-2019-170), PDB by the US  
463 Department of Energy Office of Science (7094866), DB by French Agence Nationale de la  
464 Recherche (ANR-10-LABX-25-01; ANR-11-LABX-0002-01), JD by the Ministry of Education,  
465 Youth and Sports of the Czech Republic (LM2015061), CG by a National Science  
466 Foundation Award (1655095), and AV by RFBR project 19-04-01234-a. We also thank  
467 Joanna Baker, George Butler and Ana Navarro Campoy for helpful discussions.

468 **Author contributions**

469 ASAJ and CV developed the methodology and led the writing of the manuscript. ASAJ and  
470 AM conducted the data analysis. JA, NA, DB, AB, PDB, CB, AC, JD, AG, BG, IG, CMG, HI,  
471 RJ, HK, VM, GM, LM, FEM, JEO, TS, CS, TT, GW, SW, WW, and AV contributed data. All  
472 authors contributed to manuscript revisions.

473 **Competing interests**

474 The authors declare no competing interests.